MODELING THE EVOLUTION OF CARBON INTENSITY: LINKING THE SOLOW MODEL TO THE TRANSPORT EQUATION

Pablo Garcia Sanchez and Olivier Pierrard

LIDAM Discussion Paper IRES
2025 / 06

UCLouvain

LIDAM
IRES | Louvain Institute of Data Analysis and Modeling in economics and statistics

MODELING THE EVOLUTION OF CARBON INTENSITY: LINKING THE SOLOW MODEL TO THE TRANSPORT EQUATION

PABLO GARCIA SANCHEZ AND OLIVIER PIERRARD

Abstract. While a sustained contraction of global production could lower total carbon emissions, it would hamper economic development in poorer countries, reduce living standards for low-income households in advanced economies, and heighten the risk of social unrest. Therefore, reducing carbon intensity – emissions per unit of output – appears to be the most viable and sustainable path forward. We make two contributions: one empirical and one theoretical We make two contributions: one empirical and one theoretical. Empirically, we show that the transport equation, a basic partial differential equation from physics, captures well the evolution of the distribution of carbon intensities across major economies since 1995. Theoretically, we show that in an extended Solow model with abatement capital, the distribution of carbon intensity across a continuum of economies follows the dynamics described by the transport equation. Moreover, this theory-backed version remains empirically plausible under standard parameter values. In addition, unlike its empirical counterpart, it enables projections of emissions and temperature increases under various policy scenarios, aligning closely with forecasts by leading institutions.

JEL Codes: O44, Q50.

Keywords: Carbon intensity; Transport equation; Solow model.

March 2025. Banque centrale du Luxembourg, Département Économie et Recherche, 2 boulevard Royal, L-2983 Luxembourg (contact: pablo.garciasanchez@bcl.lu, olivier.pierrard@bcl.lu).

1. Introduction

While a sustained contraction of global production could lower total carbon emissions, it would hamper economic development in poorer countries, reduce living standards for low-income households in advanced economies, and heighten the risk of social unrest. Therefore, reducing carbon intensity – emissions per unit of output – appears to be the most viable and sustainable path forward.

We make two contributions: one empirical and one theoretical. Empirically, we draw on the transport equation, a fundamental partial differential equation in physics used to model the movement of quantities, such as mass and energy. We show that, with minimal assumptions and only two parameters, this well-known equation captures very well changes in the cross-sectional distribution of carbon intensity across the world's largest economies since 1995. Moreover, it generates forecasts of global carbon emissions in 2050 that align closely with those generated by leading institutions using large and complex integrated assessment models (IAMs), including the International Energy Agency (IEA) and the Intergovernmental Panel on Climate Change (IPCC).

Theoretically, we show that the canonical Solow model, extended with abatement capital (a subject of extensive study; e.g., Xepapadeas, 2005; Siebert, 2008; Brock and Taylor, 2010), leads to a transport equation governing the cross-sectional distribution of carbon intensity across a continuum of identical economies with differing initial carbon intensities. While the theoretical version imposes stricter restrictions on the structure of the transport equation compared to its empirical counterpart, it remains empirically plausible under standard parameter values, accounting for the historical dynamics of global GDP, carbon emissions, and the distribution of carbon intensity. Moreover, coupling the transport equation with the well-established Solow model sheds light on the possible forces driving these historical patterns. For instance, we will argue that technological advancements in the production process likely played a greater role in reducing carbon intensities over recent decades than shifts in the composition of output away from agriculture and manufacturing and toward services.

Furthermore, unlike the empirical version, the theory-driven transport equation allows us to project carbon emissions and temperature increases under various policy scenarios, such as ramping up abatement efforts, accepting a global economic slowdown, or facing political backlash against climate change measures. The results align well with existing projections. For example, gradually increasing investment in abatement capital to 5% of global output by 2050 – an amount commonly estimated as necessary to support the green transition (see World Economic Forum, 2023, and references therein) – leads to carbon emissions of 13 billion tonnes by 2050, a reduction of approximately 65% compared to 2021 levels. This

closely aligns with the 12 billion tonnes projected by the International Energy Agency under the assumption that all national climate ambitions and targets are fully met (International Energy Agency, 2024).

As mentioned above, we use one of the most stylized models that captures the relationship between economic growth and the environment – the Solow model with abatement capital. Thus, the perhaps surprising relationship with the transport equation cannot be attributed to any exoticism in the underlying model. In this setup, carbon emissions arise as a by-product of production processes, while abatement capital, which is non-productive, lowers emissions per unit of output. The model does not feature optimizing behavior regarding consumption or savings; instead, the shares of output allocated to productive and abatement capital are exogenous. Furthermore, it ignores welfare damages from pollution, preventing the model from ranking the desirability of different policy scenarios. We are comfortable with these features: our aim is to show the empirical plausibility of the theory-driven transport equation by comparing its predictions with historical data and existing projections.[1]

While our focus is different, our work connects with the extensive literature that uses dynamic general equilibrium models to explore environmental issues. Due to the breadth of this field, we reference a few key contributions. Bovenberg and Smulders (1995) explore the link between environmental quality and economic growth in an endogenous growth model, emphasizing the conditions under which long-run sustainable growth is both feasible and optimal. More recently, Hassler et al. (2016) stress the choice between technologies with different impact on the quality of the environment. Acemoglu et al. (2012) and Acemoglu et al. (2016) develop endogenous growth models with clean and dirty technologies, focusing on the optimal use of carbon taxes and green subsidies. Likewise, Golosov et al. (2014) examine optimal carbon taxes, exploring their sensitivity to key factors, including the discount rate and the economic losses resulting from carbon emissions.

At this point, the reader might ask: why study the cross-sectional distribution of carbon intensities? After all, what matters to the planet is the total amount of carbon emissions, not where they come from. There are at least two reasons. First, the evolution of the cross-sectional distribution offers valuable insights into the sustainability of economic growth. For instance, a distribution that tightens around low carbon intensities might be less concerning than one that grows more diffuse, with some countries soaring to higher carbon intensities.

[1]In addition, Ackerman et al. (2009) and Stern et al. (2022) discuss the limitations and contestable assumptions of IAMs, which may undermine the effectiveness of even the largest and most complex models in welfare analysis. Pindyck (2017) echoes these concerns: '*IAM-based analyzes of climate policy create a perception of knowledge and precision that is illusory, and can fool policy-makers into thinking that the forecasts the models generate have some kind of scientific legitimacy.*' Our stylized model is unlikely to fool anyone.

Second, the geographical distribution of carbon emissions is crucial in the political economy of negotiating multilateral climate change agreements (Aldy, 2006). Hence the extensive empirical literature examining convergence in pollution per capita or per unit of output across countries (see Pettersson et al., 2014, for a throughout review of the literature). For instance, in their seminal work, Strazicich and List (2003) find that CO2 emissions per capita converged across 21 industrial economies from 1960 to 1997. More recent works by Ordas Criado and Grether (2011), Karakaya et al. (2019) and Lawson et al. (2020) apply more advanced econometric techniques and newer data sources to revisit this question. Broadly, the findings point to convergence in pollution levels among developed economies over the past few decades. Our transport equation replicates this convergence using a negative rate of decay to compress the cross-sectional distribution over time.

The reader might still wonder: why use the transport equation to model the cross-sectional distribution of carbon intensities? One reason lies in the cumulative nature of mathematics: we build on established knowledge – here, the transport equation – to tackle new challenges, such as understanding how carbon intensities evolve across countries and over time. Framing the problem this way leverages centuries of insights into waves models, providing a well-posed structure that offers clear advantages both analytically and numerically. Analytically, it ensures that our characterization of the cross-sectional distribution of carbon intensities is unique and evolves continuously with the initial conditions. Numerically, it guides us toward the most effective approximation scheme by relying on existing knowledge of finite difference methods for wave models.

Another reason to rely on the transport equation is the long tradition of using functional relationships from physics to model economic outcomes. Some of the most notable examples include: Newton's law of gravitation, applied to describe patterns of bilateral trade flows between countries (see e.g., Chaney, 2018); the heat equation, central to the Black-Scholes model (Black and Scholes, 1973); and power laws, which account for nontrivial patterns involving cities, firms, or the stock market (Gabaix, 2016).

The remainder of the paper is organized as follows. Section 2 shows that a simple, two-parameter conservative transport equation accounts for changes in the cross-sectional distribution of carbon intensity over time. Section 3 presents an extension of the Solow model with abatement capital, showing that it leads to a conservative transport equation governing the cross-sectional distribution of carbon intensity across a continuum of identical economies with varying initial carbon intensities. Section 4 validates this theory-backed transport equation empirically. Section 5 uses it to project carbon emissions and temperature increases by 2050 under different scenarios. Section 6 concludes.

2. Evolution of the cross-sectional distribution of carbon intensity

Carbon intensity, defined as the ratio of CO2 emissions per unit of GDP, has steadily declined in most regions since the mid-1990s (left panel of Figure 1). Three factors likely account for this trend (Pindyck, 2021). First, GDP composition has shifted, with a larger share now coming from services, which are often less carbon-intensive than manufacturing and agriculture. Second, technological advancements have improved energy efficiency across production and consumption, reducing overall energy demand. Lastly, investment in renewable has grown, decreasing the reliance on fossil fuels, especially coal, and making the energy mix greener.

On a more detailed scale, the right panel of the figure shows the cross-sectional distribution of carbon intensity across the 50 largest world economies in 1995, which accounted for 89% of global carbon emissions in 2021. For reasons that will soon be apparent, let us refer to this distribution as a wave. In line with the global decline in carbon intensity, the wave has shifted leftward as countries have reduced their carbon intensities. At the same time, the wave has compressed around lower carbon intensities, indicating a growing convergence among countries.[2]

These dynamics of a wave traveling sideways while simultaneously decaying (or amplifying) resemble the transport of pollutants in fluids, gas dynamics, glacier motion and even traffic flows. Thus, we model them using one of the basic differential equations in physics: the *transport equation* (see e.g., Chapter 2 in Olver, 2014, for a details). Also known as the unidirectional wave equation, the transport equation is a first-order partial differential equation of the form

$$\frac{\partial}{\partial t}u(t,x) + \frac{\partial}{\partial x}\left(F(t,x)u(t,x)\right) = 0\,, \tag{1}$$

where $F(t,x)$ is a known function. The solution $u(t,x)$ represents the concentration of a pollutant, gas, or traffic at spatial position x, or, in our context, the density of countries with carbon intensity x, at time t. Importantly, this version of the transport equation is *conservative*; that is, it ensures the total concentration $\int_x u(t,x)\,\mathrm{d}x$ remains constant over time (see Appendix A for a proof). Similar to modeling the motion of gas in a long pipe, where one expects mass conservation for gas atoms are neither created nor destroyed, modeling a density function requires that its integral remains constant.

Equation (1) can be rewritten as

$$\frac{\partial}{\partial t}u(t,x) + F(t,x)\frac{\partial}{\partial x}u(t,x) = -\frac{\partial}{\partial x}F(t,x)\,u(t,x)\,. \tag{2}$$

[2]The trends we observe across countries (lower carbon intensity and convergence) are also observed within smaller jurisdictions, such as across the 50 US states.

FIGURE 1. Dynamics of carbon intensity since 1995

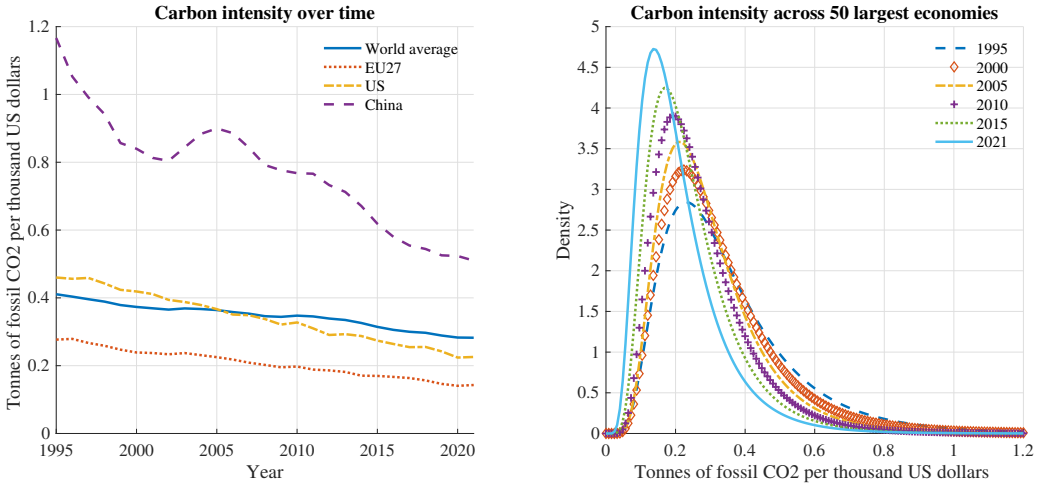

Notes. The data represent carbon intensity as the ratio of tonnes of CO2 emissions per thousand USD of GDP, with GDP expressed in Purchasing Power Parity (constant 2017 international USD). The source is Crippa et al. (EDGAR – Emissions Database for Global Atmospheric Research, 2023). The right panel examines distribution of carbon intensity among the 50 largest countries in the world (we select the countries as per their GDP in 1995, see the Penn World Table, Feenstra et al., 2015). We construct the cross-sectional distribution by fitting a log-normal distribution to the raw data. The Kolmogorov-Smirnov test does not reject the null hypothesis of a log-normal distribution at the 5% significance level for any year in the sample. Fitting alternative distributions, such as the Gamma distribution, produces identical results.

Equation (2) resembles the constant-coefficients, non-conservative form of the transport equation $u_t + cu_x = -du$. In this case, the wave moves at a constant speed c while decaying at a constant rate d.[3] Indeed, without loss of generality, let us set the initial time $t_0 = 0$. Then, $u(t,x) = v(x - ct)\,\mathrm{e}^{-dt}$ solves this simpler version, where $v(x)$ represents the initial condition, say the initial spatial distribution of the solute in the fluid. If $c = d = 0$, we have a stationary wave, whose initial profile stays frozen in place. However, if $c \neq 0$ and $d = 0$, the wave translates in space at speed c: to the right if $c > 0$, and to the left if $c < 0$. Finally, adding $d \neq 0$ means that the wave decays at rate d.

Although equation (2) is slightly more involved, it retains the same underlying intuitions. The wave speed $F(t,x)$ is no longer constant, but now depends on both time and spatial position, as does the rate of decay $\partial F(t,x)/\partial x$. Our previous discussion suggests that modeling changes in the cross-sectional distribution of carbon intensity requires $F(t,x) < 0$, indicating the wave is moving leftward, and $\partial F(t,x)/\partial x < 0$, indicating the wave is compressing around low carbon intensities. We assume the following.

Assumption 1 (Transport equation)**.** *Let* $F(t,x) = -ax\,\mathrm{e}^{-bt}$ *with* $a > 0$ *and* $b \in \mathbb{R}$.

[3]We use the notation $u_t \coloneqq \partial u(t,x)/\partial t$ and $u_x \coloneqq \partial u(t,x)/\partial x$.

Clearly, $F(t,x) < 0$ and $\partial F(t,x)/\partial x < 0$. This choice is arbitrary, and more complex specifications might better fit the data. However, our specification yields a closed-form solution to equation (2), as the next proposition shows.

Proposition 1 (Solution to the transport equation)**.** *Under Assumption 1 and given the initial condition $u(0,x) = v(x)$, the unique solution to equation* (2) *is*

$$u(t,x) = v(s)\frac{s}{x}, \quad \textit{with} \quad s = x\,\mathrm{e}^{\frac{a}{b}\left(1-\mathrm{e}^{-bt}\right)} .$$

Proof. See Appendix A. The problem is well-posed for $b = 0$, in which case we have $s = x\,\mathrm{e}^{at}$. □

Our next step is to estimate parameters a and b so that $u(t,x)$ in Proposition 1 aligns with the evolution of the carbon intensity distribution shown in the right panel of Figure 1. We proceed as follows. First, we normalize time such that $t = 0$ corresponds to 1995 and $t = 1$ corresponds to 2021. Second, we set the initial condition $u(0,x) = v(x)$ to match the observed cross-sectional distribution in 1995 (dashed blue line in the right panel of the figure). Specifically, this defines $v(x)$ as the log-normal probability density function with parameters $\mu = -1.19$ and $\sigma = 0.53$. Lastly, we use a standard quasi-Newton algorithm to minimize the distance between the observed cross-sectional distribution and $u(t,x)$ at two points in time: 2008 (corresponding to $t = 0.5$) and 2021 (corresponding to $t = 1$). The resulting parameter values are $(a^*, b^*) = (0.33, -0.80)$, with 95% confidence intervals (assuming a and b are normally distributed) of $[0.28, 0.38]$ and $[-1.1, -0.51]$, respectively. Finally, we verify that the Hessian is positive definite, confirming that the minimization problem reaches a local minimum at (a^*, b^*).

We assess the fit by comparing the model's dynamics with those observed in the data. The left panel of Figure 2 shows the full cross-sectional distribution of carbon intensity for 1995, 2008, and 2021 – the years used in the estimation process. By construction, the model and data are identical in 1995, as this year provided the initial condition. More importantly, the model closely matches the data in 2008, and nearly exactly in 2021, with both curves overlapping everywhere. Table 1 presents selected statistics for years not included in the estimation exercise. Our simple transport equation tracks well the mean, mode, and standard deviation of the cross-sectional distribution of carbon intensity over time.[4]

Emboldened by the strong performance of our transport equation at matching the past, we now ask: can it provide sensible long-term forecasts of global CO2 emissions? To address this question, we compute $u(2.11, x)$, corresponding to the model's projected cross-sectional distribution for 2050. The dashed green light in the right panel of Figure 2 shows the results. As expected, compared to 2021, the wave continues to travel leftward, compressing

[4]Tracking the mean, the mode and the standard deviation also implies reproducing the skewness, since the Pearson's first skewness coefficient is (mean-mode)/(standard deviation).

FIGURE 2. Observed and projected dynamics of carbon intensity

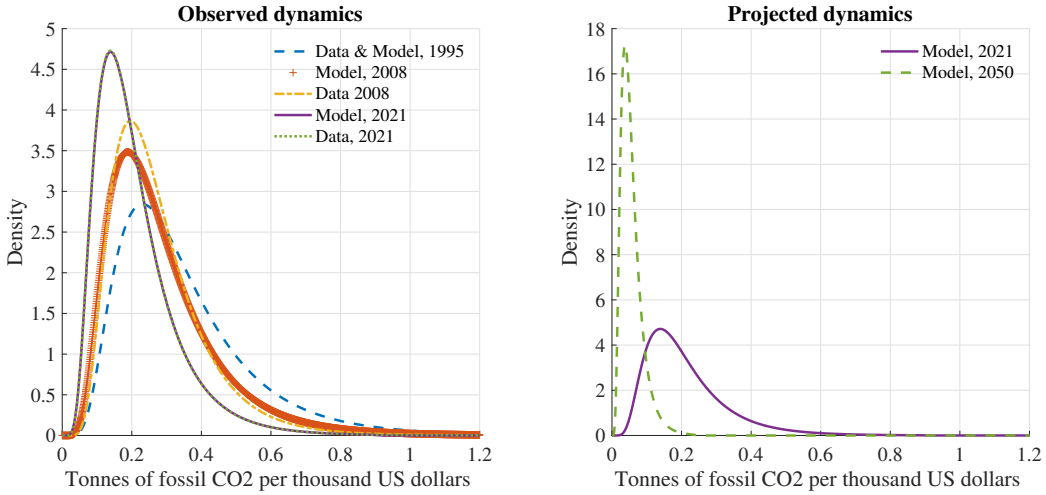

Notes. The model refers to the solution of the transport equation presented in Proposition 1, using the estimated parameters $(a^*, b^*) = (0.33, -0.80)$. Detailed information about the data can be found in Figure 1.

TABLE 1. Data vs Model: selected moments

	Mean		**Mode**		**Standard Deviation**	
	Data	Model	Data	Model	Data	Model
1995	0.35	0.35	0.23	0.23	0.19	0.19
2000	0.32	0.32	0.22	0.21	0.17	0.18
2005	0.30	0.30	0.21	0.20	0.15	0.16
2010	0.27	0.27	0.19	0.18	0.14	0.15
2015	0.24	0.24	0.17	0.16	0.13	0.13
2021	0.21	0.21	0.14	0.14	0.12	0.12

Notes. The model refers to the solution of the transport equation presented in Proposition 1, using the estimated parameters $(a^*, b^*) = (0.33, -0.80)$. Detailed information about the data can be found in Figure 1.

as it moves. By 2050, the model predicts a tightly concentrated distribution with a mean of 0.06, a mode of 0.04, and a standard deviation of only 0.03 – a fourfold reduction compared to 2021. With the carbon intensity measure in hand, we estimate global CO2 emissions in 2050 using the identity

$$\text{CO2 emissions in 2050} = \text{Carbon intensity in 2050} \times \text{GDP in 2050}.$$

Hence, given a forecast for global GDP in 2050, we approximate global CO2 emissions by multiplying the projected GDP by either the mean or the mode of our predicted carbon intensity distribution.

Table 2 presents the results. Each column reports the global CO2 emissions (in billion tonnes) projected for 2050, based on annual world GDP growth rates of 2%, 3%, and 4% from 2023 onward. Each row shows the emissions estimates using either the mean or the mode of our predicted carbon intensity distribution for 2050. For example, according to our transport equation, if world GDP grew from 2023 onward at around 3% annually, total CO2 emissions in 2050 would reach approximately 15 billion tonnes. How does Table 2 compare with projections from leading institutions? The International Energy Agency's latest estimates suggest a wide range of outcomes depending on policy efforts, with emissions in 2050 ranging from near zero under stringent climate actions to around 12 billion tonnes with moderate measures, and up to 29 billion tonnes if policies remain less ambitious (International Energy Agency, 2024). Similarly, the latest estimates from the Intergovernmental Panel on Climate Change (IPCC) suggest that limiting global warming to 1.5°C (2°C) would likely require CO2 emissions to reach 10 (20) billion tonnes in 2050 (Intergovernmental Panel on Climate Change, 2023). Lastly, the U.S. Energy Information Administration estimates that the current trajectory of the global energy system could lead to worldwide CO2 emissions of 40 billion tonnes by 2050 (U.S. Energy Information Administration, 2023).

All told, our two-parameter model's projections align with the spectrum of available estimates. One might wonder, however, whether fitting a simple linear trend to the world average carbon intensity (solid blue line in the left panel of Figure 1) could yield similar outcomes, without needing to consider our partial differential equation. The answer is no. Doing so would imply a 2050 carbon intensity of 0.15, well above our estimates. The logic is straightforward. While simple, our transport equation captures important nonlinear dynamics that help match both observed data and available projections. Specifically, the wave speed features $F(t,x) < 0$ together with $\partial F(t,x)/\partial x < 0$, implying that countries with high carbon emissions reduce them *faster* than those with low emissions. Moreover, in addition to moving leftward with varying velocity $F(t,x)$, our wave amplifies exponentially, as prescribed by $\partial F(t,x)/\partial x < 0$. These two non-linearity explain why our transport equation suggests a faster reduction in carbon intensity – and thus in total CO2 emissions – than naively extending the past trend of world average carbon intensity.

In spite of its empirical credibility, our transport equation lacks economic foundations; neither its structure nor its parameters are derived from a theoretical framework. This makes it difficult, if not impossible, to use it for policy analysis or to provide economic intuitions behind its results. However, somewhat surprisingly, a simple Solow model with abatement capital leads to a conservative transport equation of the form in equation (2). The rest of the paper justifies this statement and revisits our projections using a new theory-backed transport equation.

TABLE 2. Projected global CO2 emissions in 2050 (billion tonnes)

	World GDP growth rate		
Carbon intensity	2%	3%	4%
Mode	10.1	13.1	17.0
Mean	15.1	19.7	25.6

Notes. Each column reports the total CO2 emissions (in billion tonnes) projected for 2050, based on annual world GDP growth rates of 2%, 3%, and 4% from 2023 onward. Each row shows the emissions estimates using either the mean or the mode of our predicted carbon intensity distribution for 2050 under parameters $(a^*, b^*) = (0.33, -0.80)$.

3. Carbon emissions in the Solow model

This section extends the canonical Solow model to include abatement capital, which does not contribute to output directly but reduces carbon emissions. This setup is well-known in the environmental economics literature (see, e.g., Xepapadeas, 2005; Siebert, 2008). Thus, the resulting transport equation governing the cross-sectional distribution of carbon intensity cannot be attributed to any exoticism of the underlying model. We proceed as follows: first, we introduce the economic module, which characterizes the production technology; next, we present the environmental module, which links economic activity to carbon emissions; finally, we show how the setup leads to a transport equation governing the evolution of the cross-sectional distribution of carbon intensity.

3.1. **Economic module.**

Consider the standard constant returns to scale production function

$$Y = K^{\alpha}(AL)^{1-\alpha}\,,$$

where output Y is produced using regular capital K and labor L. Parameter $\alpha \in (0,1)$ represents the elasticity of output with respect to capital. Labor grows at a rate $n \geq 0$, while labor-augmenting technological progress, A, grows at a rate $g \geq 0$. We normalize both $L(0)$ and $A(0)$ to 1.

Suppose a fraction $s \in (0,1)$ of output is invested in regular capital, a fraction $s_a \in [0, 1-s)$ is invested in abatement capital, and the remaining fraction $1 - s - s_a$ is consumed. Although the choice of s_a is not modeled here, it might reflect some type of environmental policy choice.[5] Under the assumption that both types of capital depreciate at a rate $\delta \in (0,1)$, they evolve according to

$$\left\{ \begin{array}{rcl} \dot{K} & = & s\,Y - \delta K\,, \\ \dot{K}_a & = & s_a\,Y - \delta K_a\,, \end{array} \right.$$

[5]Moreover, the saving rate in the Solow model is exogenous. We show in Appendix B that the constant saving rate can be micro-founded using a Ramsey model with an endogenous discount rate and externalities.

with initial conditions $K(0) = K_0 > 0$ and $K_a(0) = K_{a_0} \geq 0$. As usual, we express all variables in efficiency units: $y \coloneqq Y/(AL)$, $k \coloneqq K/(AL)$, and $k_a \coloneqq K_a/(AL)$. Defining $\Delta \coloneqq n + g + \delta$, the model simplifies to

$$\begin{cases} \dot{k} = s\, k^{\alpha} - \Delta k\,, & \text{(3a)} \\ \dot{k_a} = s_a\, k^{\alpha} - \Delta k_a\,, & \text{(3b)} \\ k(0) = k_0 \coloneqq K_0\,, & \text{(3c)} \\ k_a(0) = k_{a_0} \coloneqq K_{a_0}\,. & \text{(3d)} \end{cases}$$

This first-order system of ordinary differential equations forms an autonomous initial value problem with several noteworthy properties. First, its equilibrium solution is $k^* = (s/\Delta)^{1/(1-\alpha)}$ and $k_a^* = s_a k^{*\alpha}/\Delta$. Second, since the right hand side of the system is continuously differentiable in $(k, k_a) \in \mathbb{R}_{>0} \times \mathbb{R}_{>0}$, this equilibrium solution is unique. Third, this equilibrium is asymptotically stable, as the eigenvalues of the Jacobian matrix evaluated at the equilibrium are both negative.

As mentioned earlier, one potential driver of the observed decline in carbon intensity is the shift toward a greener energy mix. To model this logic in a simple, broad manner, we allow the share s_a of output allocated to abatement capital to increase over time, reducing the share allocated to regular capital investment to keep $s_a + s$ constant.[6] In addition, we ensure that changes in s_a are sufficiently small to maintain all shares within the interval $[0, 1]$. Assumption 2 formalizes these conditions.

Assumption 2 (Rising investment rate in abatement capital)**.** *The shares of output allocated to abatement capital and to regular capital evolve by*

$$\begin{cases} \dot{s}_a &= m\,, \\ \dot{s} &= -m\,, \\ s_a(0) &= s_{a_0}\,, \\ s(0) &= s_0\,, \end{cases}$$

with $m \geq 0$, $s_0 \in (0, 1)$, and $s_{a_0} \in [0, 1 - s_0)$. We also impose that m is sufficiently small to always ensure that $s_a < 1$ and $s > 0$ during the period of time under consideration.

Under Assumption 2, the differential equation for regular capital admits a closed-form solution, as established in the next proposition.

[6]This assumption is consistent with empirical evidence indicating that the global GDP share devoted to all forms of investment has remained relatively stable over recent decades (see Section 4 for further discussion and references). An alternative approach would involve holding s constant and adjusting the share $1-(s_a+s)$ allocated to consumption instead.

Proposition 2 (Solution to differential equation for regular capital)**.** *Under Assumption 2, the system of equations* (3a) *and* (3c) *has the closed-form solution*

$$k = \left[\left(k_0^{1-\alpha} - \frac{m + s_0(1-\alpha)\Delta}{(1-\alpha)\Delta^2} \right) \mathrm{e}^{-(1-\alpha)\Delta t} + \frac{s_0}{\Delta} - \frac{m}{\Delta} \left(t - \frac{1}{(1-\alpha)\Delta} \right) \right]^{\frac{1}{1-\alpha}} .$$

Proof. See Appendix C. □

3.2. **Environmental module.** As in Xepapadeas (2005), we link gross carbon emissions X to abatement capital and output through the relationship

$$X = \Phi \left(\frac{K_a}{AL} \right) Y ,$$

where $\Phi > 0$, $\Phi' < 0$, and $\Phi'' > 0$. In words, gross emissions are proportional to output and decrease in a convex manner with respect to abatement capital. We define

$$x \coloneqq X/Y$$

as emissions per unit of GDP, or equivalently, carbon intensity (x has thus the same meaning as in Section 2), which gives

$$x = \Phi(k_a) . \tag{4}$$

We use the following simple functional form

$$\Phi(k_a) = \phi \, \mathrm{e}^{-\theta \, k_a} . \tag{5}$$

Here, $\phi > 0$ represents the scaling level of carbon intensity in the economy, and $\theta > 0$ represents the semi-elasticity of x with respect to k_a, serving as a measure of the efficiency of abatement capital. Rather than treating these as constant parameters, we assume they may change over time.

Indeed, a second potential driver of the decline in carbon intensity is the sectoral shift from carbon-intensive manufacturing and agriculture toward less carbon-intensive services. To capture this logic simply, we allow parameter ϕ to decline over time. A fall in ϕ, all else being equal, lowers carbon emissions, regardless of GDP levels, abatement capital, or its effectiveness. We assume the following.

Assumption 3 (Sectoral shift)**.** *The scaling level of carbon intensity, ϕ, evolves by*

$$\begin{cases} \dot{\phi} &= -q , \\ \phi(0) &= \phi_0 , \end{cases}$$

with $q \geq 0$ and $\phi_0 > 0$. We also impose that q is sufficiently small to always ensure that $\phi > 0$ during the period of time under consideration.

The final potential driver of the decline in carbon intensity is the technological improvements in the way we produce and use goods and services, leading to lower energy consumption. To reflect this idea in a straightforward way, we allow parameter θ to grow over time. A rise in θ, all else being equal, boosts the efficiency of abatement capital in reducing carbon intensities, thereby lowering overall emissions. We assume the following.

Assumption 4 (Efficiency gains)**.** *The efficiency of abatement capital, θ, evolves by*

$$\begin{cases} \dot{\theta} &= p\,, \\ \theta(0) &= \theta_0\,, \end{cases}$$

with $p \geq 0$ and $\theta_0 \geq 0$.

It follows from equations (3d), (4), and (5), and from Assumptions 3 and 4, that $x \in (0, \phi)$, with an initial condition $x(0) = x_0 \coloneqq \phi_0\, \mathrm{e}^{-\theta_0 k_{a_0}}$. Moreover, carbon intensity evolves by

$$\dot{x} = -x \left(\dot{\theta} k_a + \theta \dot{k}_a - \frac{\dot{\phi}}{\phi} \right). \tag{6}$$

As expected, carbon intensity decreases with a declining ϕ, an increasing θ, and an increasing k_a. By combining equation (6) with equations (3b),(4),(5), and Assumptions 2 to 4, we express $\dot{x}$ as

$$\begin{aligned} \dot{x} &= F(t,x) \\ &\coloneqq -x \left[(\theta_0 + p\,t)(s_{a_0} + m\,t)\, k^\alpha + \left(\Delta - \frac{p}{\theta_0 + p\,t} \right) \ln \frac{x}{\phi_0 - q\,t} + \frac{q}{\phi_0 - q\,t} \right], \end{aligned} \tag{7}$$

where k is given in Proposition 2. The function $F(t,x)$, known as the drift, captures the speed at which carbon intensity changes over time. This notation for $F(t,x)$ is intentional, as it aligns with our previous use of the concept in Section 2. Next subsection will aggregate individual emissions and show that the resulting distribution corresponds to a conservative-transport equation, with $F(t,x)$ representing the velocity of the distribution and the velocity gradient $\partial F(t,x)/\partial x$ (i.e., the difference in velocity between adjacent levels of carbon intensities) corresponding to its decay rate. Given its importance for our analysis, the next proposition delves into the properties of $F(t,x)$.

Proposition 3 (Properties of $F(t,x)$)**.** *The function $F(t,x)$ as defined in equation* (7) *features*

$$\begin{aligned} &\frac{\partial F(t,x)}{\partial x} = F_x(t,x) \coloneqq \frac{F(t,x)}{x} - \left(\Delta - \frac{p}{\theta_0 + p\,t} \right), \\ &\frac{\partial F(t,x)}{\partial s_0} < 0\,, \quad \frac{\partial F(t,x)}{\partial s_{a_0}} < 0\,, \quad \frac{\partial F(t,x)}{\partial p} < 0\,, \quad \frac{\partial F(t,x)}{\partial \Delta} > 0\,, \\ &\frac{\partial F_x(t,x)}{\partial s_0} < 0\,, \quad \frac{\partial F_x(t,x)}{\partial s_{a_0}} < 0\,. \end{aligned}$$

Proof. See Appendix C. □

Proposition 3 does not determine the signs of F and F_x, which are ambiguous and depend on the parametrization. However, the proposition does provide insights into the effects of several parameters. First, both the regular capital investment rate s (through a higher initial value s_0) and the abatement investment rate s_a (through a higher initial value s_{a_0}) reduce F and F_x, i.e., they decelerate the increase in carbon intensity or accelerate its decrease, particularly at higher values of x. This is not surprising, as both rates promote abatement investments – indirectly for s through higher available output, and directly for s_a. Second, faster improvements in the efficiency of abatement capital (higher p) lower the velocity of carbon intensity, making the wave shift leftward faster. Third, higher output growth or higher depreciation of capital (both resulting in a higher Δ and hence lower abatement capital) increase the velocity of carbon intensity, making the wave shift rightward faster. However, the effects of p and Δ on the velocity gradient are ambiguous.

3.3. **Distribution of carbon intensity and total carbon emissions.** We now transition from equation (7) to an equation governing the evolution of the cross-sectional distribution of carbon intensity, $u(t, x)$. To this end, we consider a mass of countries, which are identical in all respects except for their initial levels of abatement capital and, consequently, their initial carbon intensities. Specifically, we assume the following.

Assumption 5 (Initial conditions)**.** *There is a fixed mass of countries (normalized to one), each characterized by identical parameters, laws of motion, and initial conditions, except for their initial levels of abatement capital, and consequently, their initial carbon intensities. Let $v(x)$ represent this initial density of carbon intensities.*

Assumption 5 allows us to describe the evolution of the cross-sectional distribution of carbon intensities through a conservative transport equation, as shown in the next proposition.[7]

Proposition 4 (Distribution of emissions)**.** *Let $u(t, x)$ be the density of countries with carbon intensity x at time t, with the initial density $u(0, x) = v(x)$ given. Under Assumption 5, if emissions in each country evolve as described in equation* (7)*, then $u(t, x)$ is the unique solution to*

$$\begin{cases} \frac{\partial}{\partial t} u(t,x) + F(t,x) \frac{\partial}{\partial x} u(t,x) = -\frac{\partial}{\partial x} F(t,x)\, u(t,x)\,, \\ u(0,x) = v(x)\,. \end{cases}$$

Proof. See Appendix A. □

[7]Appendix D relaxes this assumption, allowing for multiple sources of heterogeneity. Crucially, our main insights remain unchanged. However, additional complexity comes at the cost of mathematical tractability: the transport equation no longer describes the distribution of carbon intensity. Instead, we need to rely on Monte Carlo simulations.

Crucially, this first-order partial differential equation is identical to equation (2) in Section 2. To briefly recap, this equation describes the transport of the initial distribution of carbon intensity, $v(x)$, with wave speed $F(t,x)$ and decay rate $\partial F(t,x)/\partial x$. As shown in Section 2, an estimated reduced form for $F(t,x)$, where $F(t,x) < 0$ and $\partial F_x(t,x)/\partial x < 0$, reproduced the data accurately and generated sensible long-term forecasts. In Section 4, we will parametrize our theoretical setup and assess whether the resulting transport equation performs similarly.

Lastly, under Assumption 5, total carbon emissions, E, follow from

$$\begin{aligned} E &= \int_0^\infty x\, Y\, u(t,x)\,\mathrm{d}x \\ &= k^\alpha\, \mathrm{e}^{(n+g)t} \int_0^\infty x\, u(t,x)\,\mathrm{d}x\,. \end{aligned}$$

where $u(t,x)$ is the density function of countries with emissions (per unit of GDP) x at time t, as given in Proposition 4.

4. Parametric illustrations

We have shown that extending the canonical Solow model with abatement capital leads to a conservative transport equation of the same form as that studied in Section 2. However, is this equation empirically valid under plausible parameter values? After confirming that it is, we use the model as a quantitative laboratory to project carbon emissions and, hence, temperature increases under various policy scenarios

4.1. **Numerical approximation scheme.** The initial value problem outlined in Proposition 4, with $F(t,x)$ defined by equation (7), does not admit a closed-form solution. Hence, we solve it using a finite difference method, replacing the derivatives in the transport equation with numerical differentiation formulae. As discussed in Proposition 3, the wave speed $F(t,x)$ can take both positive and negative values. To ensure numerical stability for both cases, we employ a standard upwind scheme, using a forward difference scheme to approximate $\frac{\partial}{\partial x}u(t,x)$ when $F(t,x) < 0$ and a backward difference scheme when $F(t,x) > 0$ (see Chapter 5 in Olver, 2014, for a detailed discussion on finite difference schemes for solving the transport equation).

4.2. **Model parametrization.** For the parameters $\{\alpha, g, n, \delta, k_0, s_{a_0}, s_0, m\}$ governing the economic module, we choose fairly standard values. We normalize one time unit to 26 years, meaning $t = 0$ corresponds to 1995 and $t = 1$ corresponds to 2021. We set the capital share, α, to 0.3 in line with the literature. According to the World Bank (Dieppe, 2021), global output per worker grew at an average annual rate of 2% from 1995 to 2018, so we set $g = 26 \times \log(1 + 0.02) \approx 0.51$. In addition, the World Development Indicators report an average growth rate of the global labor force of roughly 1.5% from 1995 to 2021, so we

set $n = 26 \times \log(1 + 0.015) \approx 0.39$. We set the annual depreciation rate of capital to 0.02, implying $\delta = -26 \times \log(1 - 0.02) \approx 0.5$. This annual rate is slightly lower than the 0.03 used in previous studies (Romer, 1989; Mankiw et al., 1992). However, using a lower value will help us better align the model's predictions with observed data.

To determine the investment rates, we use data from the International Monetary Fund's World Economic Outlook Database, which reports that the average share of global GDP allocated to investment from 1995 to 2021 was approximately 0.25, implying that $s + s_a = 0.25$. Meanwhile, data from the Organisation for Economic Co-operation and Development (OECD) shows that environment-related inventions accounted for 7.4% of total inventions in 1995 across its members, increasing to 10.4% by 2019. Based on these figures, we approximate $s_a(0) = s_{a_0} = 0.25 \times 0.07 \approx 0.018$ and $s_a(1) = 0.25 \times 0.10 \approx 0.026$, with a linear transition between these years, resulting in $m \approx 0.008$. We immediately infer $s(0) = s_0 = 0.25 - 0.018 = 0.232$.

The final parameter in the economic module is the initial stock of regular capital in efficiency units, k_0. We set k_0 to its equilibrium value, assuming that the share of output invested in regular capital remained constant (i.e., $m = 0$). That is $k_0 = k^* = (s_0/\Delta)^{1/(1-\alpha)} \approx 0.08$. This choice implies that in our numerical illustrations, GDP growth is largely driven by $n + g$, as the capital stock in efficiency units, k, barely moves given the small value of m derived earlier. This aligns with the data: according to the Penn World Tables, the mean and median growth rates of the capital stock for a sample of 138 countries from 1995 to 2019 were 3.7% and 3.2%, respectively — figures that closely match the sum of the annual growth rates of the labor force and labor-augmenting technological progress.

As for the environmental module parameters $\{\mu, \sigma, \phi_0, \theta_0, p, q\}$, we set the initial distribution of carbon intensity, $u(0, x)$, to match the observed cross-sectional distribution in 1995 (dashed blue line in the right panel of Figure 1). Specifically, we define $u(0, x) = v(x)$ as the log-normal probability density function with parameters $\mu = -1.19$ and $\sigma = 0.53$. To ensure the earlier-stated restriction $x \in (0, \phi)$ holds at the initial period, we normalize the initial scaling level $\phi_0 = 2$.[8]

We calibrate the remaining parameters to align the model with two empirical outcomes: (1) cumulative growth of global CO2 emissions of approximately 60% between 1995 and 2021; and (2) a cross-sectional distribution of carbon intensities in 2021 that resembles the solid blue line in the right panel of Figure 1. To achieve these targets, we employ a grid search method, evaluating parameter values over a predefined range to match the empirical

[8]The choice of ϕ_0 serves purely as a scaling factor; as long as it is sufficiently large to satisfy $x_0 \in (0, \phi_0)$, its level does not affect the results. For any given ϕ_0, we can adjust other parameters to yield the same outcomes.

TABLE 3. Model parametrization

Parameter	Value	Description	Parameter	Value	Description
Economic module					
α	0.30	Capital elasticity	δ	0.50	Capital depreciation
g	0.51	Productivity growth	n	0.39	Population growth
s_{a_0}	0.018	Initial abatement inv. share	m	0.008	Slope abatement inv. share
s_0	0.232	Initial capital inv. share	k_0	0.08	Initial capital
Environmental module					
μ	-1.19	Log-N initial distribution	σ	0.53	Log-N initial distribution
ϕ_0	2	Initial scaling level	q	0.08	|slope| scaling level
θ_0	80	Initial efficiency	p	120	Slope efficiency

Notes. One unit of time in our model corresponds to 26 years.

outcomes as closely as possible. This procedure yields the following values: (i) an initial efficiency $\theta_0 = 80$ for abatement capital; (ii) the slope of θ set to $p = 120$; and (iii) the absolute value of the slope of ϕ set to $q = 0.08$, implying that, had GDP and abatement efforts remained constant from 1995 to 2021, CO2 emissions would have fallen by 4% due to structural shifts toward a more service-oriented economy. Subsection 4.3.1 delves into the empirical plausibility of these values.

Table 3 summarizes our parametrization.

4.3. **Solow model-implied dynamics from 1995 to 2021.** Figure 3 compares the model-implied dynamics of global GDP, carbon emissions and carbon intensities with observed data from 1995 to 2021. Before interpreting the results, let us remind our main aim: to confirm the empirical validity of the transport equation derived from the Solow model with abatement capital. Specifically, we seek to show that, under plausible parameter values, the model generates paths for GDP, carbon emissions, and carbon intensities that are jointly consistent with observed trends.

We start with the model's strengths. First, it captures the path of global CO2 emissions and global GDP, aligning closely with observed trends. Second, it replicates the two key dynamics in the carbon intensity distribution: the leftward shift and the compression of the distribution around lower values. Specifically, the mean and standard deviation of the carbon intensity distribution are 0.35 and 0.2 in 1995, respectively, and decrease to 0.21 and 0.07 by 2021. Also, while not shown for brevity, the transition between these years is monotonic, with both the mean and the standard deviation gradually declining, as in the data.

Where does the model fall short? First, it fails to capture the steep rise in global CO2 emissions during the 2000s, instead predicting a more gradual increase. Second, the model compresses the distribution of carbon intensity too quickly compared to observed data. In

FIGURE 3. World CO2 emissions, world real GDP and carbon intensity

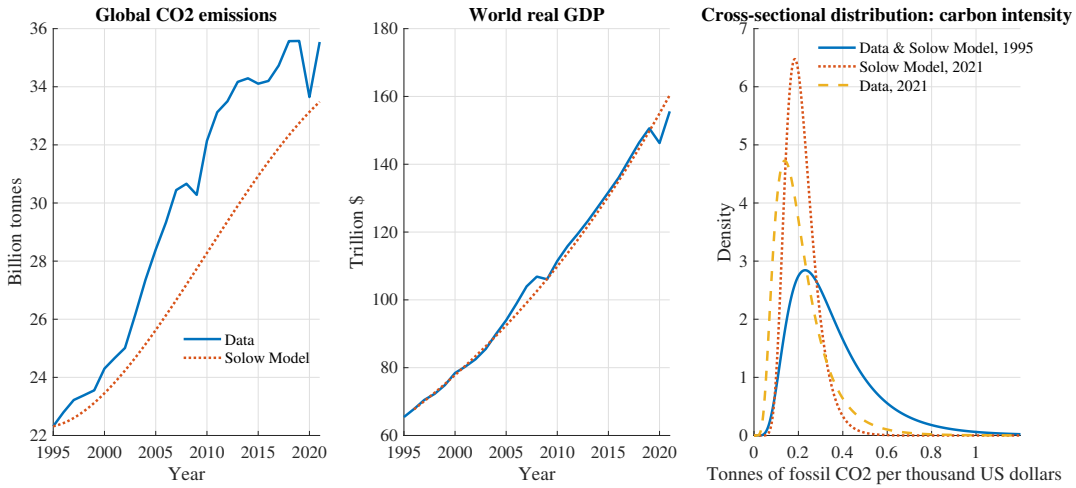

Notes. Data on world CO2 emissions, which excludes land-use change and forestry (LUCF), comes from the Climate Watch database. Real world GDP comes from the World Bank's World Development Indicators. Detailed information about the data on carbon intensity can be found in Figure 1. In the model, total CO2 emissions are given by variable E, total GDP by variable Y, and carbon intensity distribution in 2021 by $u(1, x)$.

2021, the standard deviation of carbon intensity in the data is 0.12, whereas the model underestimates it at 0.07. Finally, the model struggles to match the mode of the distribution in 2021. The mode is 0.14 in the data, but the model places it at 0.18.

Despite its shortcomings, the model matches the dynamics of global GDP, carbon emissions, and carbon intensities, supporting the empirical plausibility of the theory-backed transport equation. To further strengthen our confidence in the model and better understand its limitations, let us address two natural follow-up questions. First, do the forces underlying Figure 3 align with real-world data? Second, how do the dynamics predicted by the theory-backed transport equation compare to those of its empirical counterpart, which fits historical data more closely? We address each question in turn.

4.3.1. *Counterfactual scenarios.* The Solow model with abatement capital does a fair job at tracking carbon emissions and intensities over the past three decades. However, are the exogenous forces driving this performance empirically plausible? To address this question, we conduct a series of counterfactual exercises. In the model, lower carbon emissions result from three exogenous factors: a sectoral shift toward greener activities (captured by a declining ϕ), improvements in the efficiency of abatement capital (captured by an increasing θ), and a rising stock of abatement capital (partly induced by a rising s_a). Let us then study how

TABLE 4. Counterfactual scenarios

	2021 Global emissions	**2021 Carbon intensity distribution**	
	Billion tonnes	Mean	Standard deviation
Data	35.5	0.21	0.12
Benchmark	33.5	0.21	0.07
No sectoral shift ($q = 0$)	34.9	0.22	0.07
No efficiency gains ($p = 0$)	123	0.79	0.10
Constant investment rate ($s_a = 0$)	42.6	0.27	0.09

Notes. The first row shows the observed 2021 global carbon emissions along with the first two moments of the cross-sectional distribution of carbon intensities. The second row presents the corresponding figures in the benchmark scenario. The third, fourth, and fifth rows show the figures had ϕ, θ, or s_a remained fixed at their 1995 levels, respectively. As a remainder, in the data and the benchmark model, the mean and the standard deviation of carbon intensity were of 0.35 and 0.19 in 1995.

total emissions and the cross-sectional distribution of carbon intensities would have changed had ϕ, θ, or s_a remained fixed at their 1995 levels.

Table 4 presents the results. The first row shows the observed 2021 global carbon emissions along with the first two moments of the cross-sectional distribution of carbon intensities. The second row presents the corresponding figures in the benchmark scenario discussed earlier. Finally, the third, fourth, and fifth rows show the figures had ϕ, θ, or s_a remained fixed at their 1995 levels, respectively.

Clearly, in the model, improvements in the efficiency of abatement capital are the most significant factor driving the decline in carbon intensities and emissions (fourth row). Without these improvements, the cross-sectional distribution of carbon intensities shifts *rightward*, causing global emissions to rocket. In a distant second, the model attributes the next most significant influence to the rising share of output spent on abatement capital (fifth row). Had this share remained at its 1995 level, the model suggests a milder leftward shift in the cross-sectional distribution compared to the data, along with a significantly higher level of total emissions. Lastly, the model assigns little importance to sectoral shifts (third row), which is unsurprising given the low value of q in the benchmark calibration.

How do these outcomes relate to real-world data? Let us start with the sectoral shift toward services and away from manufacturing and agriculture, to which our model assigns little importance. This may not be as unrealistic as it initially appears. Although the services sector's share of global GDP did go up by 14 percentage points from 1970 to 2021, most of the adjustment occurred between 1970 and 1990.[9] From 1995 to 2021, the rise was only 1.5 percentage points to reach 67%. This weak increase suggests that the sectoral shift

[9]Source: United Nations Trade and Development Data Hub.

might have played a relatively limited role in recent decades, consistent with the model's assessment.

To our knowledge, no empirical data exists on the global stock of abatement capital, let alone its efficiency in reducing carbon intensities. Thus, comparing our first two counterfactuals – where θ and s_a are fixed at their 1995 levels – with real-world data is difficult. However, the notion that improvements in the efficiency of abatement capital, rather than an increase in the share of output allocated to it, play a more significant role in reducing carbon intensities seems plausible. For example, from 1995 to 2021, the share of energy generated by low-carbon sources increased by just 3.3 percentage points, reaching 17.7%.[10]

On the whole, drawing direct parallels between the model and empirical data is challenging, for the notion of abatement capital is too stylized to have a clear counterpart in reality. Yet, that technological advances have played a major role in reducing carbon intensities is not hard to believe.[11]

4.3.2. *Comparison with the empirical transport equation.* Earlier, we showed that the theory-driven transport equation struggles to match the mode and standard deviation of the 2021 distribution (refer to Figure 3). To understand the reasons behind this, we compare the dynamics predicted by the theory-driven transport equation with those of its empirical counterpart, which aligns more closely with historical data. The most natural way to make this comparison is by analyzing their respective characteristic curves. This is due to a fundamental property of wave models (Olver, 2014): the value of the solution $u(t, x)$ at a given time t and position x depends only on its initial value along the characteristic curve that passes through (t, x). In simpler terms, the characteristic curves in our context address the question: what would be the 2021 carbon intensity of a country that had a carbon intensity of x_0 in 1995?

By definition, a characteristic curve for our transport equation solves

$$\frac{\mathrm{d}x}{F(t,x)} = \mathrm{d}t\,, \tag{8}$$

[10]Source: Energy Institute - Statistical Review of World Energy (2024).

[11]The argument that technological advances have done and will continue to do – almost – all the work is often put forward by policymakers or business leaders seeking to avoid additional efforts. While technological advances hold significant potential, relying solely on them to address climate change can be risky, as demonstrated in the next section. Indeed, we show that the 'business as usual scenario' (which extends the past trends, including the strong technological progresses) is not not enough to reduce significantly emissions at the 2050 horizon; and that a more balanced approach (which adds policy changes and/or behavioral shifts to the 'business as usual scenario') is needed.

FIGURE 4. Characteristic curves of the conservative transport equation (2)

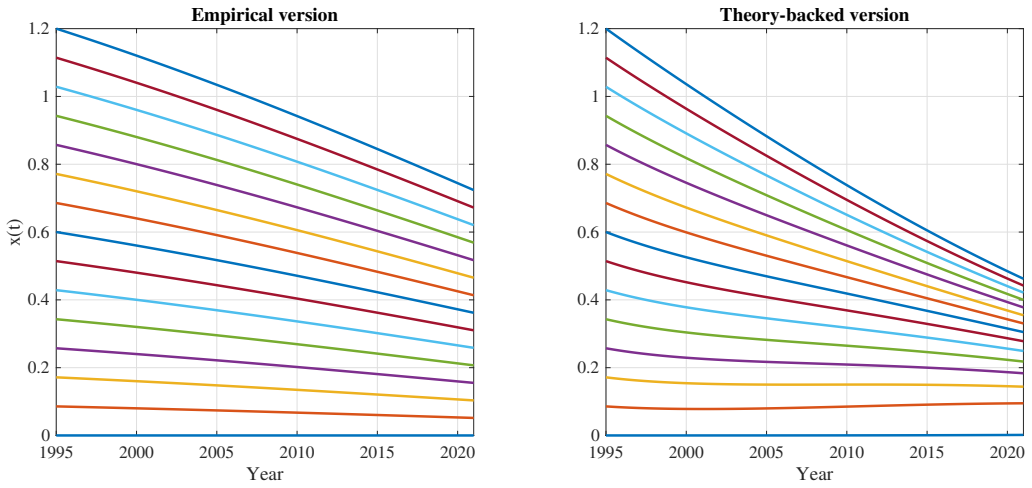

Notes. Characteristic curves solve the initial value problem of the ordinary differential equation (8). Each initial condition defines a distinct characteristic curve.

with initial values $t = 0$ and $x = x_0$. Each initial value x_0 defines a distinct characteristic curve. In the empirical transport equation, the drift function $F(t, x)$ is specified by Assumption 1, while in the theory-driven version, it is defined by equation (7). In the former case, equation (8) does accept a closed-form solution,[12] though the expression is not particularly enlightening. In the latter case, equation (8) does not accept a closed-form solution and must be solved numerically. Figure 4 plots the characteristic curves in both cases for a wide range of initial conditions, x_0.

These curves track a country's carbon intensity over time, given its initial value x_0. While in reality, two countries could reach the same carbon intensity at the same time despite differing starting points, none of our models allow for this scenario, because such an outcome would violate the uniqueness of the solution to the transport equation. This is why characteristic curves in the figure never intersect.

As shown in Section 2, the empirical transport equation tracks the cross-sectional distribution of carbon intensity over time very well. Therefore, deviations between the characteristic curves of the theory-backed transport equation and those of the empirical transport equation result in a worse data fit. Broadly, both sets of characteristic curves behave similarly, particularly in that they decrease (almost) everywhere. This monotonicity is ensured in the empirical model – where $F(t, x) < 0$ by construction –, but not in the theoretical setup (see Proposition 3). In the theory-driven transport equation, although the data does not show a

[12]This occurs because Assumption 1 imposes that F is multiplicatively separable in t and x, such that we can have x only on the left-hand side and t only on the right-hand side, and integrate both sides from their respective initial values

perfectly monotonic decline in carbon intensities, it avoids large swings as well (see Figure 1).

Nonetheless, the theory-driven version does differ from its empirical counterpart in two main ways. First, for high values of x_0 (e.g., a country like China), the characteristic curves in the theory-backed transport equation are much steeper than those in the empirical transport equation. In contrast, for low values of x_0 (e.g., a country in Western Europe), the curves are not steep enough, and may even increase at some point. Together, these factors explain why the theory-backed transport equation struggles to match the mode and standard deviation of the 2021 distribution. Specifically, the mode does not fall enough (0.18 in the Solow model vs. 0.14 in the data), as countries with initially low carbon intensities reduce them too little. At the same time, the standard deviation falls too much (0.07 vs. 0.12), as countries with initially high carbon intensities reduce them too much.

To conclude, we are confident that, however stylized, the Solow model with abatement capital and its associated transport equation align well with past data. Hence, we now use it to explore the possible effects of different abatement efforts on global carbon emissions and, consequently, on temperature increases. While we keep a pedagogical focus – acknowledging that our model is too stylized for rigorous quantitative projections, let alone to compute 'optimal' policies – our simple projections will prove surprisingly close to those made by leading institutions using much larger and more complex models.

5. Projections 2021-2050

In this final section, we explore what our Solow model reveals about global carbon emissions and, by extension, temperature increases over the next two and a half decades under varying levels of efforts. Specifically, we consider four scenarios, all starting from the 2021 cross-sectional distribution of carbon intensity observed in the data (solid blue line in the right panel of Figure 1). The first is a *business-as-usual* case, where the parameters governing carbon intensities, $\{\phi, \theta, s_a\}$, continue to change at the same rates as between 1995 and 2021; that is, $q = 0.08$, $p = 120$, and $m = 0.008$. The second scenario reflects a green *investment boom*, where the share of output invested in abatement capital rises faster over time (i.e., $m = 0.0216$), reaching 5% by 2050 (compared to 3.5% in the business-as-usual scenario).[13] The third scenario considers *zero growth*, where labor augmenting productivity stagnates (i.e., $g = 0$), and so does global GDP per capita. The final scenario represents a

[13]Estimates of the cost of the green transition vary widely, ranging from $100 trillion to $300 trillion by 2050. For context, current global annual GDP is approximately $100 trillion. Conservative estimates suggest required green investments of 4–5% of global GDP annually, while more ambitious projections place the figure at 7–8% (see World Economic Forum, 2023, and references therein).

backlash against abatement efforts, which stop abruptly (i.e., $q = p = m = 0$) at the beginning of the time horizon. In this case, we have no more sectoral shift, efficiency improvement or further effort in investment (for instance, the share of investment in abatement capital remains at its 2021 level, that is 2.6%).

The left panel of Figure 5 compares global carbon emissions in each scenario. As anticipated, the Solow model's projections align closely with those from leading institutions. For the *business-as-usual* scenario, for instance, the model predicts carbon emissions of 28 billion tonnes by 2050. This is strikingly close to the 29 billion tonnes projected by the International Energy Agency's Stated Policies Scenario (STEPS), which reflects the ongoing trajectory of the energy system based on existing climate policies and measures as well as those that are under development (International Energy Agency, 2024). Similarly, the *investment boom* scenario, which projects carbon emissions of 13 billion tonnes by 2050, closely mirrors the 12 billion tonnes projected in the International Energy Agency's more stringent Announced Pledges Scenario (APS). The latter examines the outcome if all national announced ambitions and targets are fully met.

In turn, the *zero growth* scenario stresses how the planet does not care about ratios (carbon intensities); it cares only about absolutes (carbon emissions). While engineering a permanent global economic slowdown is probably not an appealing prospect, it does lead to a dramatic collapse in carbon emissions by 2050. Lastly, the *backlash* scenario is literally off the chart, with carbon emissions in 2050 surging to 150 billion tonnes.

We do not attempt to rank the desirability of these scenarios; our model is too stylized for such judgments.[14] Instead, we content ourselves with showing that a simple Solow model with abatement capital – relying on just a handful of parameters and functional forms – produces plausible forecasts that can complement and provide insights into the results of larger, more complex models.

To hammer this point home, let us turn from carbon emissions to temperature increases. In line with the approach of this paper, we use the simplest possible mapping between these variables, as presented in Hassler et al. (2016) and developed by Matthews et al. (2009). Briefly, let the parameter CCR, which stands for Carbon-Climate-Response, be the change in global mean temperature over some period interval $\mathrm{d}t > 0$ per unit of carbon emissions

[14]Even the most complex models likely share this limitation. Pindyck (2017) convincingly argues that large macro-climate models suffer from fundamental flaws. For instance, crucial inputs such as the damage function and the parameters governing climate sensitivity are often arbitrary, rendering these models 'close to useless' for welfare analysis. Stern et al. (2022) express strong concerns about the limitations of these models too.

FIGURE 5. World CO2 emissions, world real GDP and carbon intensity

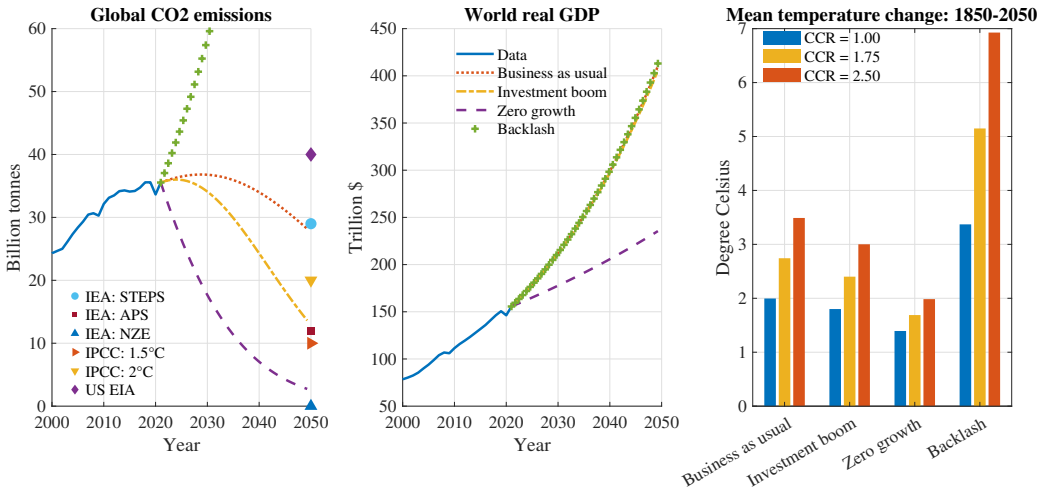

Notes. Left panel. The IEA:STEPS scenario reflects the International Energy Agency's business-as-usual projections. The IEA:APS scenario (Announced Pledges Scenario) explores outcomes if all national energy and climate targets, including net-zero goals, are achieved fully and on time. The IEA:NZE scenario assumes net-zero emissions by 2050 (International Energy Agency, 2024). The IPCC: 1.5°C (2°C) scenario outlines the emissions reductions needed by 2050 to limit global warming to 1.5°C (2°C) above pre-industrial levels according to the Intergovernmental Panel on Climate Change (2023). US EIA projects emissions conditional on the current trajectory of the global energy system (U.S. Energy Information Administration, 2023). Right panel. CCR stands for carbon-climate response, which measures the change in the global mean temperature over a specified time interval per unit of fossil carbon emissions released into the atmosphere during the same period. The CCR is likely (90% probability) to range between 1 and 2.5°C per billion tonnes of carbon emissions (Matthews et al., 2012).

over that interval. Formally,

$$CCR = \frac{T(t+\mathrm{d}t) - T(t)}{\int_t^{t+\mathrm{d}t} E(u)\,\mathrm{d}u},$$

where T denotes global mean temperature and E represents carbon emissions. While the value of CCR is unknown (see Pindyck, 2013, for details), Matthews et al. (2012) suggests that a 90% confidence interval falls between 1 and 2.5°C per billion tonnes of emissions. By inserting the projected carbon emissions paths from the left panel of Figure 5 into the above equation, with $CCR \in [1, 2.5]$, we approximate the temperature increase from 2021 to 2050. For easier interpretation, and noting that global average temperatures have already risen by

roughly 1°C since the pre-industrial era,[15] we add this 1°C to our projections and report the temperature increase in 2050 relative to the pre-industrial baseline.

The right panel of Figure 5 shows the results for the best-case, worst-case, and midpoint values of CCR in each of our scenarios. Broadly, the model's carbon paths do not generate outlandish temperature increases, suggesting that the 2050 emissions levels are plausible and that the paths to those levels are reasonable too. For example, the *business-as-usual* scenario suggests a global temperature rise exceeding 2°C above pre-industrial levels. This aligns with the findings of the IPCC, which in its recent reports highlights that without significant policy action, global temperature increases in the second half of the 21st century are likely to range from 2.1°C to 3.4°C above pre-industrial levels (Intergovernmental Panel on Climate Change, 2023). Similarly, the *zero growth* scenario, whose 2050 carbon emissions are 3 billion tonnes, suggests a likely average temperature increase above pre-industrial levels ranging from 1.4 to 2°C. This resembles the IPCC's assessment that, to have a 50% chance of limiting global warming to 1.5°C above pre-industrial levels, 2050 carbon emissions must fall below 10 billion tonnes. Lastly, our simple model stresses that if a *backlash* against abatement efforts does take hold, a catastrophic future should not be dismissed—an outcome that aligns with the wide acceptance of the risks posed by insufficient climate policy action.

6. Concluding Remarks

Understanding how the cross-sectional distribution of carbon intensity evolves over time is important in addressing climate change. Empirically, we show that the transport equation captures the evolution of the distribution of carbon intensities across major economies since 1995. Theoretically, we show that in an extended Solow model with abatement capital, the distribution of carbon intensity across a continuum of economies follows the dynamics described by the transport equation. Moreover, this theory-backed version remains empirically plausible under standard parameter values.

Our theoretical setup has three limitations that merit further research. First, it assumes exogenous shares of output allocated to abatement and productive capital, leaving the model vulnerable to the Lucas critique. Addressing this limitation would require defining agents' objective functions and incorporating optimizing behavior. Second, the model treats the effectiveness of abatement capital in reducing carbon emissions as exogenous, whereas it likely depends on endogenous factors such as resources allocated to R&D. Introducing endogenous technical change could provide a more realistic framework. Third, the model assumes that an economy's choices do not influence other economies, an assumption that may not hold in practice. For instance, the voluntary nature of international climate agreements might lead to 'free-riding', where some countries benefit from reduced greenhouse gas emissions

[15]Source: NOAA National Centers for Environmental Information.

without sharing the associated costs. Capturing these strategic interactions would require the inclusion of differential games.

References

Acemoglu, D., Aghion, P., Bursztyn, L., and Hemous, D. (2012). The Environment and Directed Technical Change. *American Economic Review*, 102(1):131–166.

Acemoglu, D., Akcigit, U., Hanley, D., and Kerr, W. (2016). Transition to Clean Technology. *Journal of Political Economy*, 124(1):52–104.

Ackerman, F., DeCanio, S. J., Howarth, R. B., and Sheeran, K. (2009). Limitations of integrated assessment models of climate change. *Climatic Change*, 95(3):297–315.

Aldy, J. E. (2006). Per capita carbon dioxide emissions: Convergence or divergence? *Environmental and Resource Economics*, 33(4):533–555.

Black, F. and Scholes, M. (1973). The pricing of options and corporate liabilities. *Journal of Political Economy*, 81(3):637–654.

Bovenberg, A. L. and Smulders, S. (1995). Environmental quality and pollution-augmenting technological change in a two-sector endogenous growth model. *Journal of Public Economics*, 57(3):369–391.

Brock, W. and Taylor, M. (2010). The Green Solow model. *Journal of Economic Growth*, 15(2):127–153.

Chaney, T. (2018). The Gravity Equation in International Trade: An Explanation. *Journal of Political Economy*, 126(1):150–177.

Crippa, M., Guizzardi, D., Schaaf, E., Monforti-Ferrario, F., Quadrelli, R., Risquez Martin, A., Rossi, S., Vignati, E., Muntean, M., Brandao De Melo, J., Oom, D., Pagani, F., Banja, M., Taghavi-Moharamli, P., Köykkä, J., Grassi, G., Branco, A., and San-Miguel, J. (2023). *GHG emissions of all world countries – 2023*. Publications Office of the European Union.

Dieppe, A., editor (2021). *Global Productivity: Trends, Drivers, and Policies*. World Bank, Washington, DC.

Feenstra, R. C., Inklaar, R., and Timmer, M. P. (2015). The Next Generation of the Penn World Table. *American Economic Review*, 105(10):3150–82.

Gabaix, X. (2016). Power Laws in Economics: An Introduction. *Journal of Economic Perspectives*, 30(1):185–206.

Golosov, M., Hassler, J., Krusell, P., and Tsyvinski, A. (2014). Optimal Taxes on Fossil Fuel in General Equilibrium. *Econometrica*, 82(1):41–88.

Hassler, J., Krusell, P., and Smith, A. (2016). Environmental Macroeconomics. In Taylor, J. B. and Uhlig, H., editors, *Handbook of Macroeconomics*, volume 2 of *Handbook of Macroeconomics*, pages 1893–2008. Elsevier.

Intergovernmental Panel on Climate Change (2023). *Climate Change 2023: Synthesis Report*. IPCC, Geneva, Switzerland.

International Energy Agency (2024). *World Energy Outlook 2024*. Paris, France.

Karakaya, E., Alataş, S., and Yılmaz, B. (2019). Replication of Strazicich and List (2003): Are CO2 emission levels converging among industrial countries? *Energy Economics*,

82(C):135–138.

Lawson, L. A., Martino, R., and Nguyen-Van, P. (2020). Environmental convergence and environmental kuznets curve: A unified empirical framework. *Ecological Modelling*, 437:109289.

Mankiw, N. G., Romer, D., and Weil, D. N. (1992). A Contribution to the Empirics of Economic Growth. *The Quarterly Journal of Economics*, 107(2):407–437.

Matthews, H. D., Gillet, N. P., Stott, P. A., and Zickfeld, K. (2009). The proportionality of global warming to cumulative carbon emissions. *Nature*, 459:829–833.

Matthews, H. D., Solomon, S., and Pierrehumbert, R. (2012). Cumulative carbon as a policy framework for achieving climate stabilization. *Philosophical Transactions of the Royal Society A: Mathematical, Physical and Engineering Sciences*, 370(1974):4365–4379.

Olver, P. J. (2014). *Introduction to Partial Differential Equations*. Springer International Publishing, 2014 edition.

Ordas Criado, C. and Grether, J.-M. (2011). Convergence in per capita CO2 emissions: A robust distributional approach. *Resource and Energy Economics*, 33(3):637–665.

Pettersson, F., Maddison, D., Acar, S., and Söderholm, P. (2014). Convergence of Carbon Dioxide Emissions: A Review of the Literature. *International Review of Environmental and Resource Economics*, 7(2):141–178.

Pindyck, R. S. (2013). Climate Change Policy: What Do the Models Tell Us? *Journal of Economic Literature*, 51(3):860–872.

Pindyck, R. S. (2017). The Use and Misuse of Models for Climate Policy. *Review of Environmental Economics and Policy*, 11(1):100–114.

Pindyck, R. S. (2021). What We Know and Don't Know about Climate Change, and Implications for Policy. *Environmental and Energy Policy and the Economy*, 2(1):4–43.

Romer, P. (1989). Capital accumulation in the theory of long run growth. In Barro, R. J., editor, *Modern Business Cycle Theory*, pages 51–127. Harvard University Press, Cambridge, MA.

Siebert, H. (2008). *Economics of the Environment*. Springer Books. Springer.

Stern, N., Stiglitz, J., and Taylor, C. (2022). The economics of immense risk, urgent action and radical change: towards new approaches to the economics of climate change. *Journal of Economic Methodology*, 29(3):181–216.

Strazicich, M. and List, J. (2003). Are CO 2 Emission Levels Converging Among Industrial Countries? *Environmental & Resource Economics*, 24(3):263–271.

U.S. Energy Information Administration (2023). International energy outlook 2023.

World Economic Forum (2023). Costing the earth: What will it take to make the green transition work? Accessed: 2024-11-28.

Xepapadeas, A. (2005). Economic growth and the environment. In Maler, K. G. and Vincent, J. R., editors, *Handbook of Environmental Economics*, chapter 23, pages 1219–1271.

Elsevier.

Appendix A. Transport equation

A.1. **Conservative transport equation.** We take the conservative transport equation (1)

$$\frac{\partial}{\partial t}u(t,x) + \frac{\partial}{\partial x}\left(F(t,x)u(t,x)\right) = 0\,,$$

with $(t,x) \in \mathbb{R}_{\geq 0} \times \mathbb{R}_{\geq 0}$. The initial condition is $u(0,x) = v(x)$ with $\int_0^\infty v(x)\,\mathrm{d}x = 1$. We moreover impose $u(t,0) = 0$ and $\lim_{x\to\infty} u(t,x) = 0$. We need to show that

$$\frac{\mathrm{d}}{\mathrm{d}t}\int_0^\infty u(t,x)\,\mathrm{d}x = 0\,,$$

i.e. that the quantity $\int_x u(t,x)\,\mathrm{d}x$ is conserved over time. Using the definition of the conservative transport equation and the boundary conditions, we have

$$\begin{aligned}\frac{\mathrm{d}}{\mathrm{d}t}\int_0^\infty u(t,x)\,\mathrm{d}x = \int_0^\infty \frac{\partial}{\partial t}u(t,x)\,\mathrm{d}x &= -\int_0^\infty \frac{\partial}{\partial x}\left(F(t,x)\,u(t,x)\right)\,\mathrm{d}x \\ &= -\left[F(t,x)\,u(t,x)\right]_{x=0}^{x=\infty} = 0\,.\end{aligned}$$

Given that the initial quantity is 1 (initial condition), this quantity is conserved through time.

A.2. **Proof for Proposition 1.** First we, compute the characteristics curves of the transport equation (2) for each initial conditions $t = 0$ and $x = s \geq 0$. They are solutions of

$$\frac{\mathrm{d}x}{F(t,x)} = \mathrm{d}t\,.$$

Using Assumption 1 and integrating each side from the initial conditions gives

$$-a\int_0^t \mathrm{e}^{-bt}\,\mathrm{d}t = \int_s^x \frac{\mathrm{d}x}{x}\,,$$

which gives $s = x\,\mathrm{e}^{\frac{a}{b}\left(1-\mathrm{e}^{-bt}\right)}$.

Second, we compute the solutions of the transport equation (2) along each characteristics. The solutions must respect

$$-\frac{\mathrm{d}u}{F_x\,u} = \mathrm{d}t\,,$$

where $F_x \coloneqq \partial F(t,x)/\partial x$. Using Assumption 1 and integrating each side from the initial conditions gives

$$a\int_0^t \mathrm{e}^{-bt}\,\mathrm{d}t = \int_{u(0,s)}^{u(t,x)} \frac{\mathrm{d}u}{u}\,.$$

The solution is $u(t,x) = v(s)\frac{s}{x}$, where we make use of $u(0,s) = v(s)$.

A.3. **Proof for Proposition 4.** We know equation (7)

$$\frac{\mathrm{d}x}{\mathrm{d}t} = F(t,x)\,,$$

with $(t,x) \in \mathbb{R}_{\geq 0} \times \mathbb{R}_{\geq 0}$. We define $u(t,x)$ as the density function of x and we impose $u(t,0) = 0$ and $\lim_{x\to\infty} u(t,x) = 0$. We have to show that

$$\frac{\partial}{\partial t}u(t,x) + \frac{\partial}{\partial x}\left(F(t,x)u(t,x)\right) = 0\,.$$

To do so, let us take any function $f(t,x) : \mathbb{R}_{\geq 0} \times \mathbb{R}_{\geq 0} \longmapsto \mathbb{R}$ which is $\mathcal{C}^1$ in both arguments. Then

$$\begin{aligned}
\mathrm{d}f(t,x) &= \frac{\partial f(t,x)}{\partial t}\,\mathrm{d}t + \frac{\partial f(t,x)}{\partial x}\,\mathrm{d}x \\
&= \frac{\partial f(t,x)}{\partial t}\,\mathrm{d}t + \frac{\partial f(t,x)}{\partial x}\,F(t,x)\,\mathrm{d}t \\
&= \left(\frac{\partial f(t,x)}{\partial t} + \frac{\partial f(t,x)}{\partial x}\,F(t,x)\right)\,\mathrm{d}t\,.
\end{aligned}$$

Taking expectations on all x gives

$$\begin{aligned}
\frac{\mathbb{E}_x\,\mathrm{d}f(t,x)}{\mathrm{d}t} &= \mathbb{E}_x\,\frac{\partial f(t,x)}{\partial t} + \mathbb{E}_x\,\frac{\partial f(t,x)}{\partial x}\,F(t,x) \\
&= \int_0^\infty \frac{\partial f(t,x)}{\partial t}\,u(t,x)\,\mathrm{d}x + \int_0^\infty \frac{\partial f(t,x)}{\partial x}\,F(t,x)\,u(t,x)\,\mathrm{d}x\,.
\end{aligned}$$

Moreover, we have

$$\begin{aligned}
\frac{\mathbb{E}_x\,\mathrm{d}f(t,x)}{\mathrm{d}t} = \frac{\mathrm{d}\,\mathbb{E}_x\,f(t,x)}{\mathrm{d}t} &= \frac{\mathrm{d}}{\mathrm{d}t}\int_0^\infty f(t,x)\,u(t,x)\,\mathrm{d}x \\
&= \int_0^\infty \frac{\mathrm{d}}{\mathrm{d}t}\left(f(t,x)\,u(t,x)\right)\,\mathrm{d}x \\
&= \int_0^\infty \frac{\partial f(t,x)}{\partial t}\,u(t,x)\,\mathrm{d}x + \int_0^\infty f(t,x)\,\frac{\partial u(t,x)}{\partial t}\,\mathrm{d}x\,.
\end{aligned}$$

By equating the two above expressions, we obtain

$$\int_0^\infty \frac{\partial f(t,x)}{\partial x}\,F(t,x)\,u(t,x)\,\mathrm{d}x = \int_0^\infty f(t,x)\,\frac{\partial u(t,x)}{\partial t}\,\mathrm{d}x\,.$$

Integrating by part the left-hand side, and remembering that $u(t,0) = 0$ and $\lim_{x\to\infty} u(t,x) = 0$ gives

$$-\int_0^\infty f(t,x)\,\frac{\partial}{\partial x}\left(F(t,x)\,u(t,x)\right)\,\mathrm{d}x = \int_0^\infty f(t,x)\,\frac{\partial u(t,x)}{\partial t}\,\mathrm{d}x\,.$$

Since this equation must hold for any function $f(t,x)$, we get

$$-\frac{\partial}{\partial x}\left(F(t,x)\,u(t,x)\right) = \frac{\partial u(t,x)}{\partial t}\,.$$

Appendix B. From Ramsey to Solow

In the Solow model, the saving rate s is exogenous. We now assume it is endogenous (Ramsey problem) and write the following Hamiltonian

$$H = \ln c + \epsilon\left((1-s_a)k^\alpha - c - \Delta k\right) ,$$

with c representing the consumption and ϵ the shadow price associated to the budget constraint. All other variable and parameters are similar to the Solow version. The first-order necessary conditions are given by $H_c = 0$, $H_k = -\dot{\epsilon} + \rho\,\epsilon$ and $H_\epsilon = \dot{k}$, where ρ is the discount rate. This gives the following system of differential equations

$$\begin{cases} \dfrac{\dot{q}}{q} = (\rho + \Delta) - (1-s_a)\,\alpha\,k^{\alpha-1} , & \text{(9a)} \\ \dot{k} = (1-s_a)k^\alpha - \dfrac{1}{q} - \Delta k . & \text{(9b)} \end{cases}$$

We assume that agents take ρ as given, although it is time-varying according to

Assumption 6 (Time-varying discount rate and externality)**.** *The discount rate evolves as* $\rho = (1-s-s_a)\,r - (1-\alpha)\Delta$*, with* $r \coloneqq \alpha k^{\alpha-1}$*. When solving the Hamiltonian, agents take* ρ *as given.*

The evolution of ρ is an externality: agents do not realize that by changing the level of capital, they also modify their discount. Moreover, we observe that the discount is proportional to r with a factor $1-s-s_a$, i.e. when the interest rate r increases, the discount rate is higher; and that $\rho > 0 \Leftrightarrow (1-s-s_a)\,r > (1-\alpha)\Delta$. It is easy to show that under Assumption 6, $q = k^{-\alpha}/(1-s-s_a)$ is solution of (9a) and equation (9b) becomes

$$\dot{k} = s\,k^\alpha - \Delta k ,$$

which is equivalent to equation (3a) obtained from the Solow model. In other words, in a Ramsey economy under Assumption 6, the share of output invested in capital is constant and equal to s. Note that our calibration (see Table 3) implies that ρ is always positive and relatively stable throughout our simulation period, and corresponds to an average yearly discount of 1.5%. Figure 6 plots its evolution.

Appendix C. Solow model

C.1. **Proof for Proposition 2.** We need to solve equation (3a) under initial condition (3c) and under Assumption 2, that is we need to solve $\dot{k} = (s_0 - mt)k^\alpha - \Delta k$ with $k(0) = k_0$. Differential equations in this form are called Bernoulli Equations and the solution is

$$k^{1-\alpha}\,\mathrm{e}^{(1-\alpha)\Delta t} = (1-\alpha)\int (s_0 - mt)\,\mathrm{e}^{(1-\alpha)\Delta t}\,\mathrm{d}t + C ,$$

FIGURE 6. Evolution of the discount rate (on a yearly basis) over time

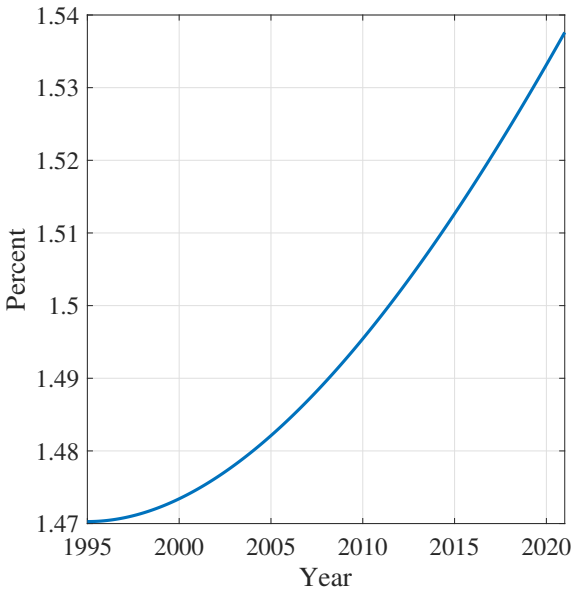

Notes. The discount rate ρ is given by Assumption (6). Since one unit of time in the model corresponds to 26 years, we transform ρ into the yearly discount ρ_y using the formula $\mathrm{e}^{-\rho} = (1-\rho_y)^{26}$.

where C is a constant of integration. Solving the right-hand side integral and simplifying gives

$$k^{1-\alpha} = \frac{s_0}{\Delta} - \frac{m}{\Delta}\left(t - \frac{1}{(1-\alpha)\Delta}\right) + C\,\mathrm{e}^{-(1-\alpha)\Delta t}\,.$$

We find the constant of integration by imposing $k(0) = k_0$, that is

$$C = k_0^{1-\alpha} - \frac{m + s_0(1-\alpha)\Delta}{(1-\alpha)\Delta^2}\,.$$

Combining the above two equations proves Proposition 2.

C.2. **Proof for Proposition 3.** We successively prove the different properties included in the proposition.

- Computing $F_x(t,x)$ is straightforward.
- $\frac{\partial F(t,x)}{\partial s_0} = -x\alpha(\theta_0 + pt)(s_{a_0} + mt)k^{\alpha-1}\underbrace{\frac{\partial k}{\partial s_0}}_{>0} < 0$
- $\frac{\partial F(t,x)}{\partial s_{a_0}} = -x(\theta_0 + pt)k^{\alpha} < 0$
- $\frac{\partial F(t,x)}{\partial p} = -x\left(ts_a k^{\alpha} - \frac{\theta_0}{\theta^2}\underbrace{\ln\frac{x}{\phi}}_{<0}\right) < 0$

- $\frac{\partial F(t,x)}{\partial \Delta} = -x\left(\theta s_a \alpha k^{\alpha-1} \underbrace{\frac{\partial k}{\partial \Delta}}_{<0} + \underbrace{\ln \frac{x}{\phi}}_{<0}\right) > 0$
- $\frac{\partial F_x(t,x)}{\partial s_0} = \frac{\partial F(t,x)}{\partial s_0} \frac{1}{x} < 0$
- $\frac{\partial F_x(t,x)}{\partial s_{a_0}} = \frac{\partial F(t,x)}{\partial s_{a_0}} \frac{1}{x} < 0$

Appendix D. Heterogeneity in productive capital

The baseline model treats countries as identical except for their initial carbon intensities. While this assumption allows us to describe the evolution of carbon intensities using a conservative transport equation, it overlooks other potential differences. For example, countries likely vary in their levels of productive capital in efficiency units, $k(0)$. This section addresses this limitation by introducing a second layer of heterogeneity, allowing for differences in both productive capital in efficiency units and carbon intensities.

Importantly, the Solow model's predictions regarding the distribution of carbon intensity remain almost unchanged, stressing the robustness of our findings. However, this additional layer of complexity comes at the cost of mathematical tractability: our two-dimensional transport equation no longer describes the distribution of carbon intensity. Instead, we need to rely on Monte Carlo simulations.

D.1. **Data.** As mentioned in the main text, our analysis takes 1995 as the initial time point ($t = 0$) and focuses on the 50 largest economies. To introduce heterogeneity in $k(0)$, we first compute its empirical counterpart and then assess its relationship with the carbon intensities of these economies in 1995. Were productive capital in efficiency units and carbon intensity positively correlated, negatively correlated, or orthogonal in 1995?

To our knowledge, no measure of productive capital in efficiency units is available for a wide range of countries. Therefore, we approximate it as the ratio of capital stock to population, with both variables sourced from the Penn World Table (Feenstra et al., 2015). That is, as in the main text, we normalize labor-augmenting productivity in 1995 to 1, $A(0) = 1$, while allowing both $K(0)$ and $L(0)$ to vary across countries. The left panel of Figure 7 plots our approximation of $k(0)$ against $x(0)$ for the largest 50 world economies in 1995. Notably, both series show little correlation, with a p-value (≈ 0.4) indicating insufficient evidence to reject the hypothesis of no correlation between $x(0)$ and $k(0)$. Fitting a log-normal multivariate distribution to both series further confirms this, with the estimated covariance approaching zero.

D.2. **Carbon intensity wave.** Since we can no longer describe the distribution of carbon intensity using the conservative transport equation, we approximate it using Monte Carlo methods. Specifically, we simulate a large number of countries, N, as follows:

FIGURE 7. Productive capital in efficiency units and carbon intensities in 1995

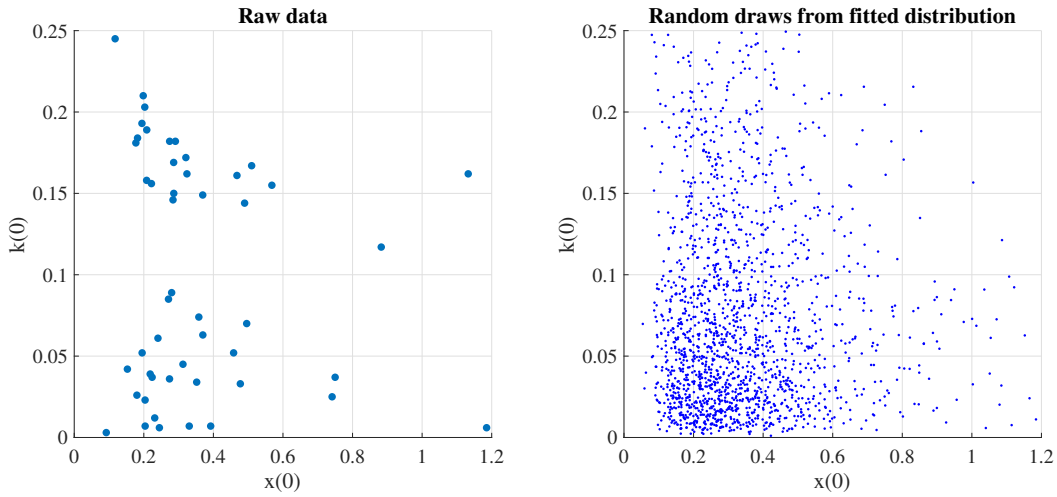

Notes. Left panel: Productive capital in efficiency units against carbon intensity across the 50 largest economies in 1995. Variable $k(0)$ is approximated as the ratio of capital stock to population in 1995. Both variables are sourced from the Penn World Table (Feenstra et al., 2015). The capital stock is expressed in constant 2017 national prices and measured in millions of units. Carbon intensity is the ratio of tonnes of CO2 emissions per thousand USD of GDP, with GDP expressed in Purchasing Power Parity (constant 2017 international USD). The source is Crippa et al. (EDGAR – Emissions Database for Global Atmospheric Research, 2023). The right panel displays 2000 random draws generated by fitting a log-normal multivariate distribution to the raw data shown in the left panel.

(1) For each $n \in N$, we draw initial conditions $\{x(0), k(0)\}$ from the fitted log-normal multivariate distribution described earlier.[16] Random draws from this distribution are illustrated in the right panel of Figure 7.
(2) For each $n \in N$, we compute $k(t)$ for all $t \in [0, 1]$ using Proposition 2. We then calculate $k_a(t)$ from its law of motion (equation (3b)) and determine $x(t)$ from equation (4).

After obtaining $x(t)$ for all $n \in N$ and $t \in [0, 1]$, we construct the cross-sectional distribution by fitting a log-normal distribution to the simulated data (consistent with the approach used for the observed data). The Kolmogorov-Smirnov test does not reject the null hypothesis of a log-normal distribution at the 5% significance level for any $t \in [0, 1]$.

Figure 8 compares the carbon intensity wave predicted by the model with two layers of heterogeneity, using the same calibration as in the main text (Table 3), to the wave observed in the data. Broadly, the extended model captures the evolution of the carbon intensity wave well. It accounts for the gradual leftward shift and the compression around low carbon

[16]The resulting mean of $k(0) \approx 0.12$ across the N countries is slightly higher than the baseline model's value, where all countries share $k(0) \approx 0.08$. However, as this discrepancy does not significantly affect the results, we retain it for simplicity and transparency.

FIGURE 8. Carbon intensity wave under two layers of heterogeneity

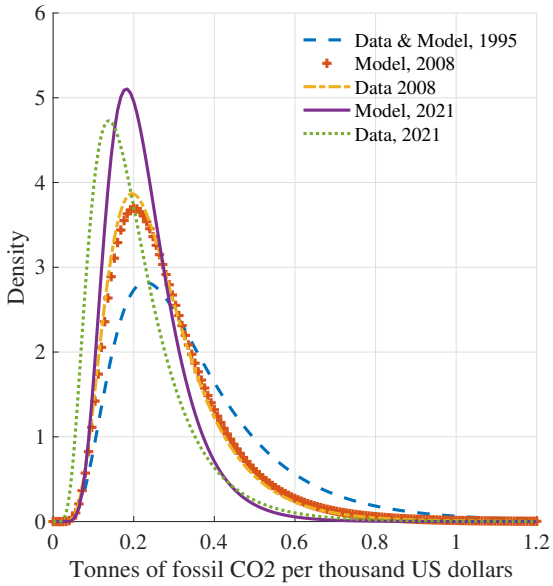

Notes. Model refers to the Solow model with two layers of heterogeneity in both productive capital in efficiency units and carbon intensities.

intensities. Also, similar to the baseline setup, it struggles to match the mode of the carbon intensity wave in 2021, predicting a mode that is too high.

Overall, the Solow model's ability to match the carbon intensity wave is not due to the assumption that countries are identical except for their initial carbon intensities. Introducing additional sources of heterogeneity does not diminish its performance and may even enhance it. However, additional complexity comes at the cost of mathematical tractability.

INSTITUT DE RECHERCHE
ÉCONOMIQUES ET SOCIALES

Place Montesquieu 3
1348 Louvain-la-Neuve

ISSN 1379-244X D/2025/3082/06

UCLouvain

IRES | LIDAM
Louvain Institute of Data Analysis and Modeling in economics and statistics